Precision in Musculoskeletal imaging: Utilizing Dixon method to Distinguish Non-Neoplastic from Neoplastic lesions

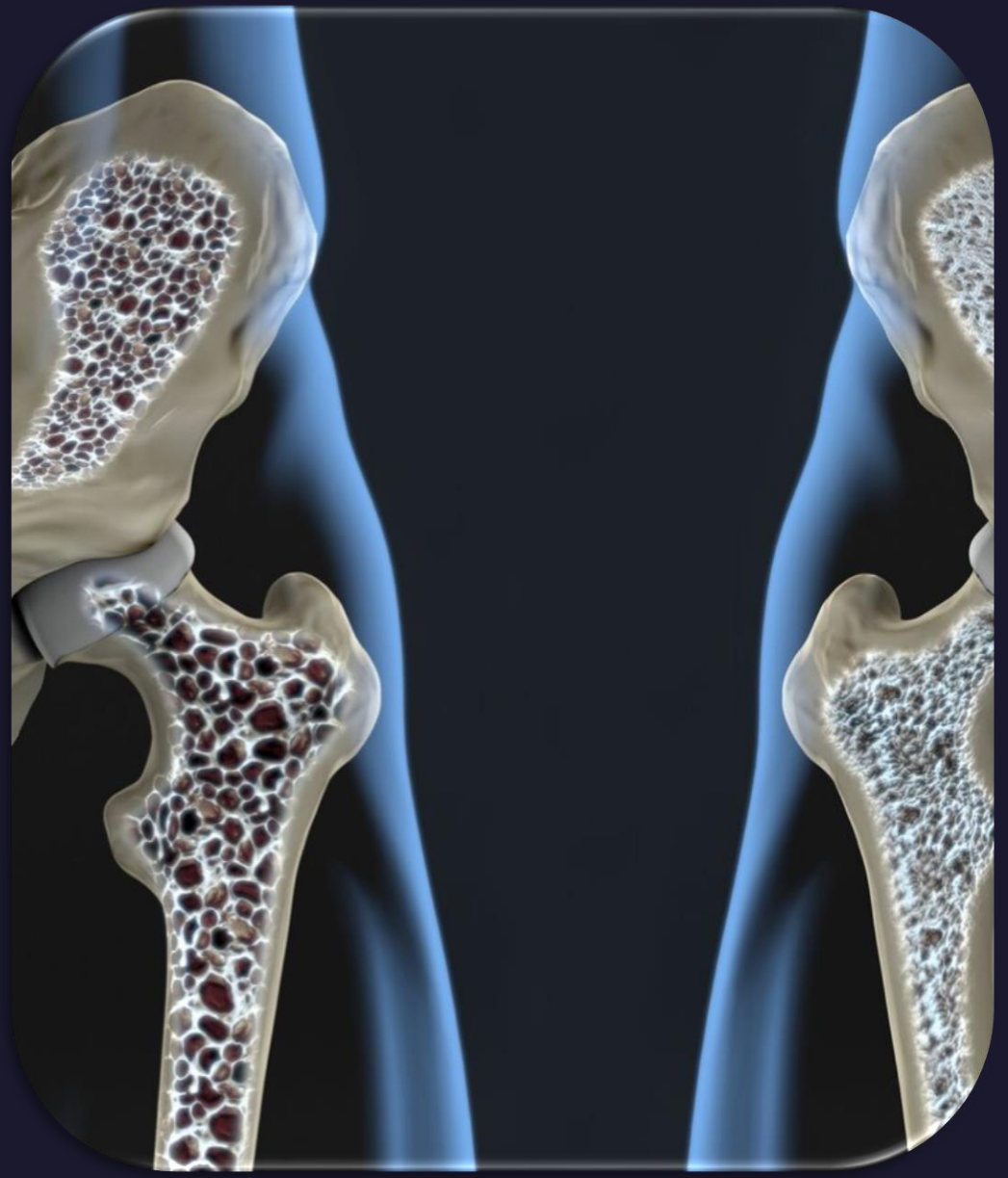

Ehsan Kazemi[1], Azadeh Rastegr[2]

MRI Radiographer, North–West Anglia NHS Foundation Trust, UK

MRI Radiographer, Afarinesh Imagining Centre, IRI

Achieving Excellence in Radiography Education and Research, 20-21 November 2024, Birmingham, UK

Learning outcomes

- The composition and roles of red and yellow marrow
- Physiological differences between non-neoplastic and neoplastic lesions
- Signal Suppression techniques in MRI
- Limitations of routine MRI sequences in MSK imaging
- Physical principles of Dixon and its diagnostic accuracy in MSK imaging
- A case study

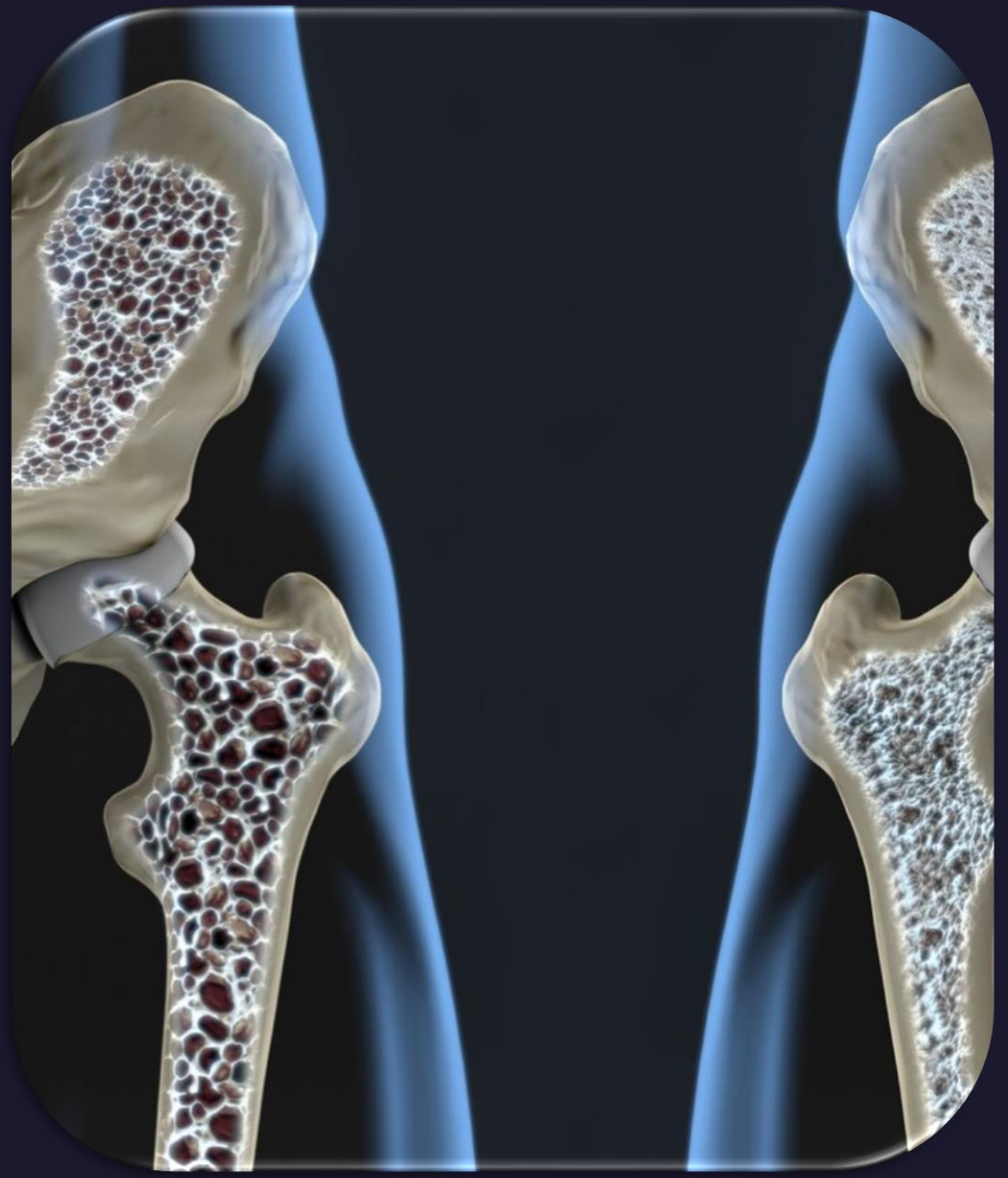

Bone marrow development and contents

In the last 3-month before the birth and after birth, **Red marrow** plays a vital role in Haemopoiesis.

INTRAMEDULLARY COMPOSITION OF **RED MARROW** VS. **YELLOW MARROW**

Red marrow		Yellow marrow
Triglycerides (fat), 40%	intramedullary fluid, 40%	Triglycerides (fat), 80%
Haempoietic cell, 20%		intermedullary fluid, 20%

(Jahanvi and Kelkar, 2021) (Omoumi, 2022)

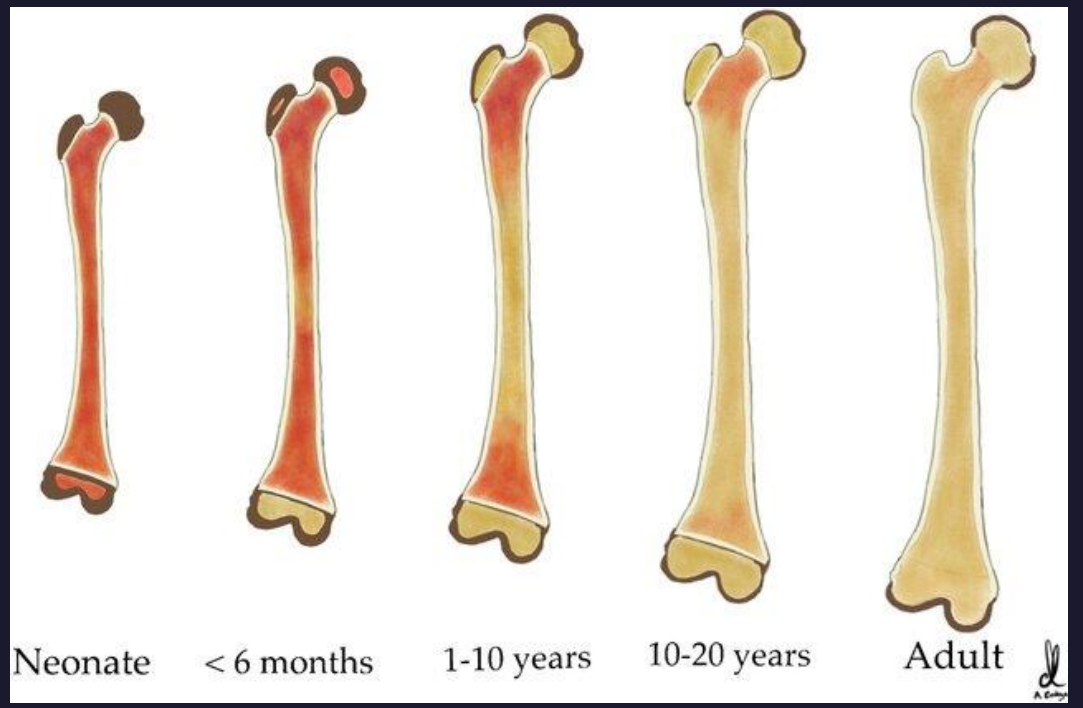

(Alexander, Laor and Bedoya, 2023)

Marrow Disorders

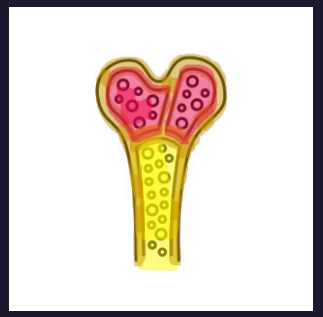

Normal
Bone marrow

Non-neoplastic lesions

Benign Neoplastic lesions

Malignant Neoplastic lesions

Non-neoplastic	Benign neoplastic	**Malignant neoplastic**
Bone abscess	Aneurysmal bone cyst	Chondrosarcoma
Bone infarct	Atypical haemangioma	Chordoma
Cystic marrow infarct	Benign notochordal tumour	Ewing sarcoma
Fibrous dysplasia	Chondroblastoma	Giant cell carcinoma (malignant)
Insufficiency fracture	Fibrous cortical defect	Leukaemia
Intraosseous ganglion	Giant cell carcinoma (benign)	Metastasis
Osteomyelitis	Non-occyfying fibroma	Myeloma
Paget's disease	Osteoma	Osteosarcoma
Post-traumatic marrow sclerosis	Simple bone cyst	Plasmacytoma
Reactive marrow oedema	Schwannoma	Pleomorphic sarcoma
Red marrow hyperplasia	Enchondroma	Round cell carcinoma
Schmorl's node		Spindle cell sarcoma

(Kohl et al., 2014) (Saifuddin et al., 2021) (Douis et al., 2016) (Van Vucht et al., 2021)

Routine musculoskeletal MRI sequences

In T1-W imaging, it is hard to precisely delineate **intramedullary borders of bone tumours** from extensive peritumoral inflammation or abundant red marrow.

(Shiga et al. 2013)

In T1-W+Contrast imaging, the enhancement can be **exaggerated** by the inflammatory responses around the detected lesion.

(Verstraete and Lang, 2000)

Other fat-suppression techniques such as **STIR** and **SPAIR** cannot be used for contrast-enhancement imaging.

(Kenneally et al., 2015)

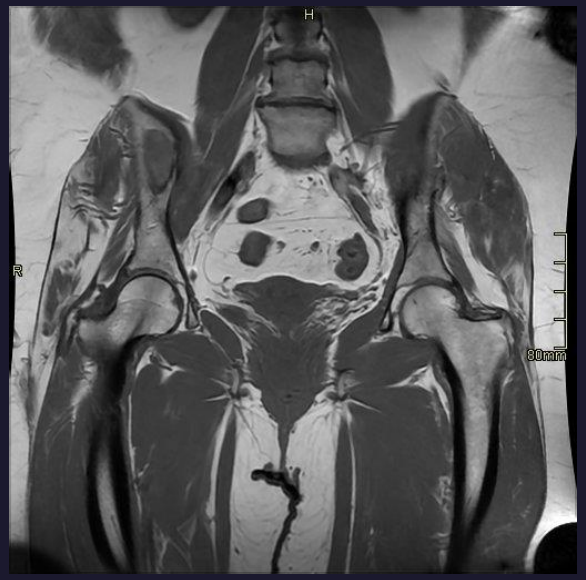

Coronal T1-Weighted of R.t femur

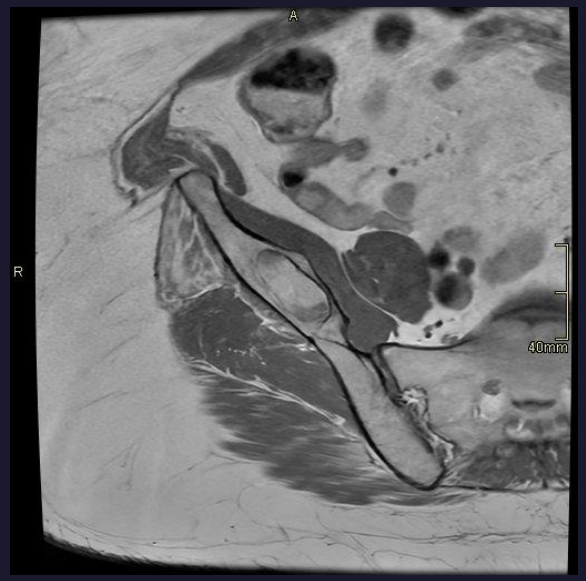

Axial T1-Weighted of R.t femur

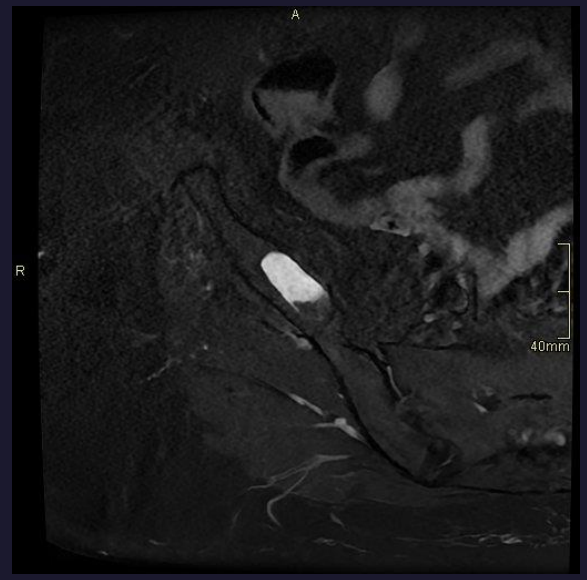

Axial STIR of R.t femur

Physical Principles in Dixon Method

$$S_{OP} = Water_{signal} - Fat_{signal}$$

$$S_{IP} = Water_{signal} + Fat_{signal}$$

$$S_{WO} = \frac{S_{IP} + S_{OP}}{2}$$

$$S_{FO} = \frac{S_{IP} - S_{OP}}{2}$$

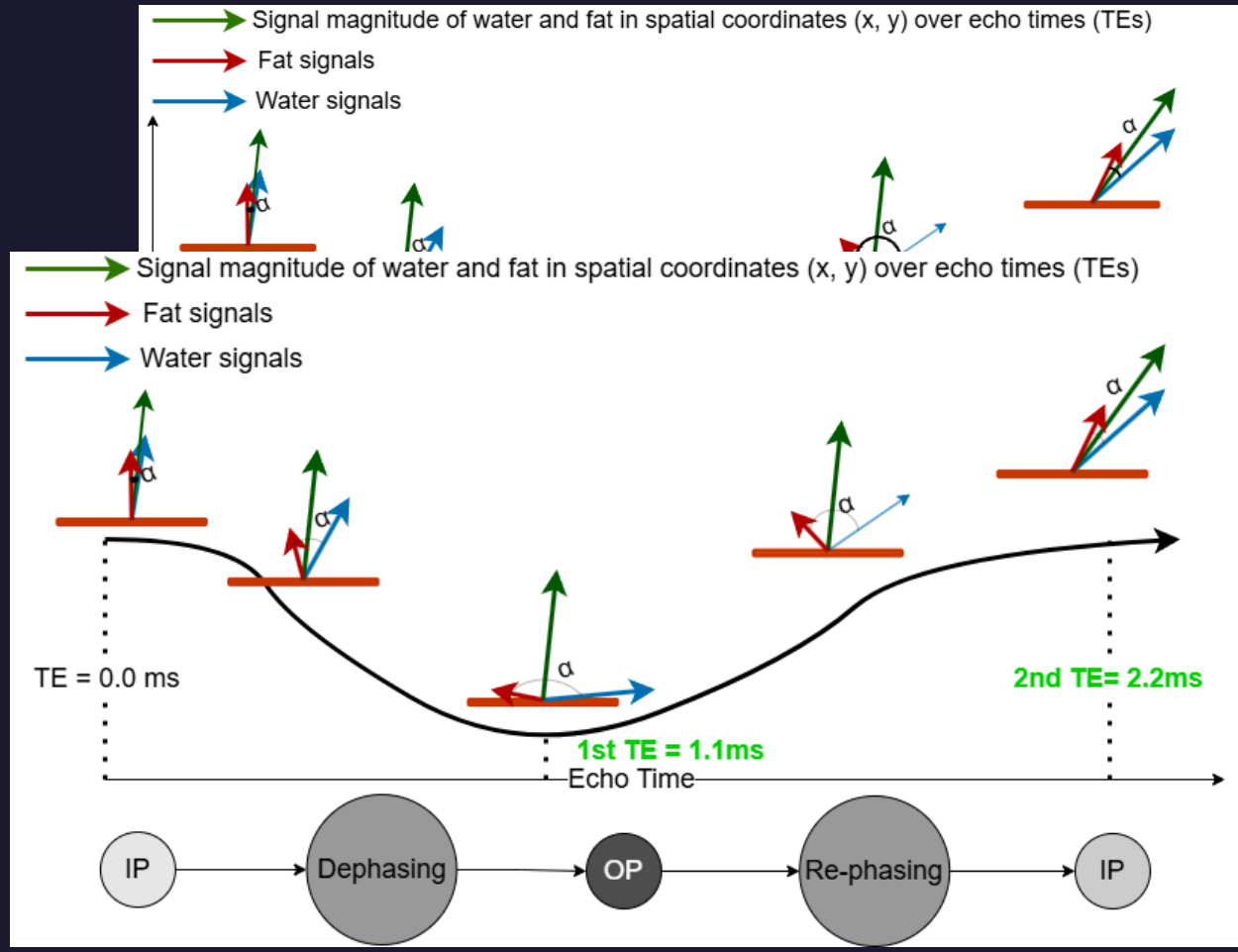

Percentage of Signal Intensity Drop (%SI Drop)

We searched seven academic databases:

1. Pub med
2. EBSChost
    1. CINHAL
    2. Academic Search Ultimate
    3. MEDLINE Complete
3. Ovid Library
    1. Ovid Emcare
    2. Embase
    3. Mediline

$$\%SI\ drop = \left[\frac{SI_{IP} - SI_{OP}}{SI^{IP}}\right] \times 100$$

Magnetic field strength:	%SI Drop in Non-neoplastic lesions	%SI Drop in Neoplastic lesion
1.5T	>20%	<20%
3.0T	>25%	<25%

We selected 11 articles (;4 primary+7 secondary research papers) based on inclusion & exclusion criteria.

Diagnostic value of %SI Drop in Dixon method

Study name	Object of study %	Sensitivity %	Specificity %	PPV %	NPV %	Accuracy %
Douis et al., 2016 (n=57)	Using T1W GRE Dixon to distinguish non-neoplastic from neoplastic (benign + malignant) lesions % SI drop (non-neoplastic)= 36.3% % SI drop (malignant lesions) = 3.3-4.0%	91.70	72.70	47.80	97.10	82.50
Kohl et al., 2014	To assess %SI drop between IP and OP images of T1W FSPGR to classify marrow lesions.	100	61	75	100	82
Saifuddin et al., 2021 (n=85)	Detecting non-neoplastic lesions with T1W GRE Dixon % SI drop (non-neoplastic)= 33.9-34.1%	66.70	88.10	61.9	90.9	84.70
	Detecting non-neoplastic lesions with **T2W FSE Dixon** % SI drop = 40.7-42.1%	72.20	85.10	58.3	92.1	83.50
	Detecting non-neoplastic lesions with T1W GRE Dixon % SI drop (benign lesions) = 7.8-12.7% % SI drop (malignant lesions) = -9.0-4.0%	72.20	89.60	63.2	92.2	84.70
	Detecting neoplastic (benign + malignant) lesions with **T2W GRE Dixon** % SI drop (benign lesions) = 14.4-15.4% % SI drop (malignant lesions) = 3.3-4.0%	77.80	86.60	59.1	93.4	83.50
Van Vucht et al., 2021 (n=174)	Using T1W GRE Dixon to distinguish non-neoplastic from neoplastic (benign + malignant) lesions % SI drop (non-neoplastic) = 36.6% % SI drop (benign lesions) = 3.19% % SI drop (malignant lesions) = 3.24%	65.90	94.60	80.6	89.1	87.40
	Using T1W GRE Dixon to distinguish benign neoplastic from malignant neoplastic lesions	9.10	98.40	85.7	51.2	53.10

The pooled sensitivity, specificity, and accuracy of T1-W Dixon imaging to distinguish non-neoplastic from neoplastic (benign & malignant) lesions were 85.86%, 76.1%, and 83.96% respectively

Case Study

$$\%SI\ drop = \left[\frac{SI_{IP} - SI_{OP}}{SI^{IP}}\right] \times 100$$

$$\%SI\ drop_{min} = \left[\frac{90.5 - 2.82}{90.5}\right] \times 100$$

$$\%SI\ drop = \mathbf{96.88\%}$$

$$\%SI\ drop_{mean} = \left[\frac{336.9 - 51.11}{336.9}\right] \times 100$$

$$\%SI\ drop = \mathbf{84.83\%}$$

$$\%SI\ drop_{max} = \left[\frac{550.36 - 298}{550.36}\right] \times 100$$

$$\%SI\ drop = \mathbf{45.85\%}$$

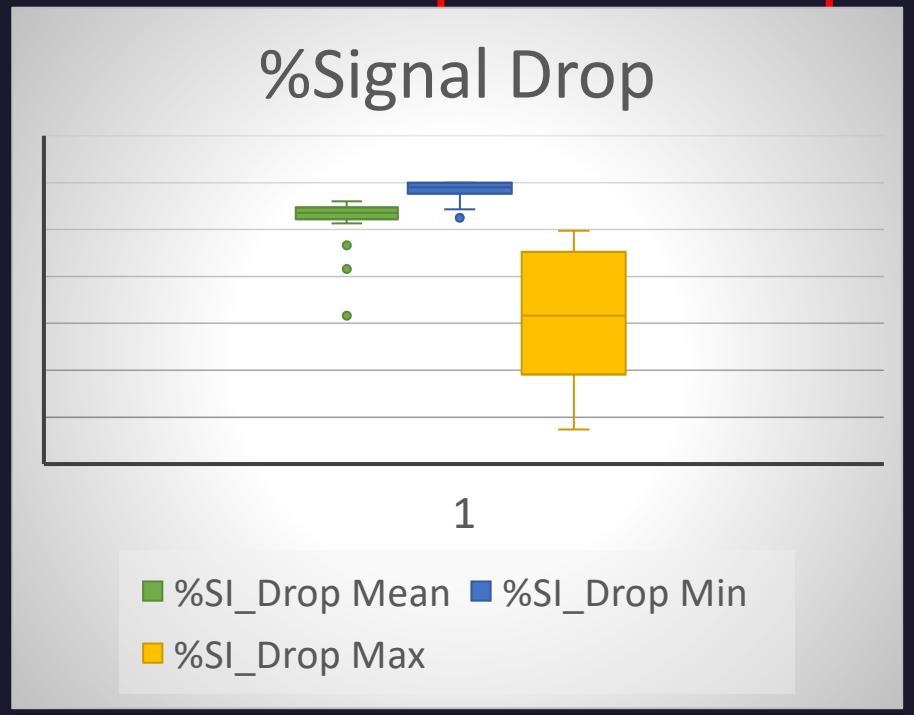

Magnetic field strength	%SI Drop in Non-neoplastic lesions	%SI Drop in Neoplastic lesions
1.5T	>20%	<20%
3.0T	>25%	<25%

Fibrous dysplasia;

Non-neoplastic lesion

Conclusion

- When routine MRI sequences are used in conjunction with the Dixon method, the diagnostic capability of MRI to differentiate between non-neoplastic and neoplastic lesions is enhanced.

- The Dixon method provides multiple image sets (OP, IP, WO, and FO) within a single acquisition, more homogenous fat suppression, and allowing for both pre- and post-contrast imaging (; unlike other CSI techniques, such as STIR and SPAIR).

- Quantitative data derived from the Dixon method can facilitate more definitive interpretation of bone marrow lesions, thus improving patient management.

- The use of the Dixon method can reduce the need for additional invasive procedures, such as bone biopsies and contrast-enhanced imaging, particularly in cases of non-neoplastic lesions.

- However, bone biopsy may still be necessary to differentiate intermediate lesions (;malignant vs. benign neoplastic).

References:

- Jahanvi, V. and Kelkar, A. (2021) 'Chemical shift imaging: An indispensable tool in diagnosing musculoskeletal pathologies', SA journal of radiology, 25(1), pp. 2061 Available at: 10.4102/sajr.v25i1.2061.
- Patrick Omoumi (2022) 'The Dixon method in musculoskeletal MRI: from fat-sensitive to fat-specific imaging ', Skeletal Radiology, 51(7), pp. 1365–1369 Available at: 10.1007/s00256-021-03950-1.
- Alexander, K.M., Laor, T. and Bedoya, M.A. (2023) 'Magnetic resonance imaging protocols for pediatric acute hematogenous osteomyelitis', Pediatric radiology, 53(7), pp. 1405–1419 Available at: 10.1007/s00247-022-05435-2.
- Dale, B.M., Brown, M.A., 1955 and Semelka, R.C. (2015) MRI: basic principles and applications. Fifth edn. Hoboken, NJ; Chichester, West Sussex: Wiley Blackwell.
- Shiga, N.T., Del Grande, F., Lardo, O. and Fayad, L.M. (2013) 'Imaging of primary bone tumors: determination of tumor extent by non-contrast sequences', Pediatric radiology, 43(8), pp. 1017–1023 Available at: 10.1007/s00247-012-2605-x.
- Verstraete, K.L. and Lang, P. (2000) 'Bone and soft tissue tumors: the role of contrast agents for MR imaging', European Journal of Radiology, 34(3), pp. 229–246 Available at: 10.1016/S0720-048X(00)00202-3.
- Kenneally, B.E., Gutowski, C.J., Reynolds, A.W., Morrison, W.B. and Abraham, J.A. (2015) 'Utility of opposed-phase magnetic resonance imaging in differentiating sarcoma from benign bone lesions', Journal of bone oncology, 4(4), pp. 110–114 Available at: 10.1016/j.jbo.2015.10.001.

References:

- Kohl, C.A., Chivers, F.S., Lorans, R., Roberts, C.C. and Kransdorf, M.J. (2014) 'Accuracy of chemical shift MR imaging in diagnosing indeterminate bone marrow lesions in the pelvis: review of a single institution’s experience', Skeletal radiology, 43(8), pp. 1079–1084 Available at: 10.1007/s00256-014-1886-6.

- Saifuddin, A., Shafiq, H., Malhotra, K., Santiago, R. and Pressney, I. (2021) 'Comparison of in-phase and opposed-phase T1W gradient echo and T2W fast spin echo dixon chemical shift imaging for the assessment of non-neoplastic, benign neoplastic and malignant marrow lesions', Skeletal radiology, 50(6), pp. 1209–1218 Available at: 10.1007/s00256-020-03663-x.

- Douis, H., Davies, A.M., Jeys, L. and Sian, P. (2016) 'Chemical shift MRI can aid in the diagnosis of indeterminate skeletal lesions of the spine', European radiology, 26(4), pp. 932–940 Available at: 10.1007/s00330-015-3898-6.

- Van Vucht, N., Santiago, R., Pressney, I. and Saifuddin, A. (2021) 'Role of in-phase and out-of-phase chemical shift MRI in differentiation of non-neoplastic versus neoplastic benign and malignant marrow lesions', British journal of radiology, 94(1119), pp. 20200710 Available at: 10.1259/bjr.20200710.

- Kumar, N.M., Ahlawat, S. and Fayad, L.M. (2018) 'Chemical shift imaging with in-phase and opposed-phase sequences at 3 T: what is the optimal threshold, measurement method, and diagnostic accuracy for characterizing marrow signal abnormalities?', Skeletal radiology, 47(12), pp. 1661–1671 Available at: 10.1007/s00256-018-2999-0.

THANKS!

Any questions?

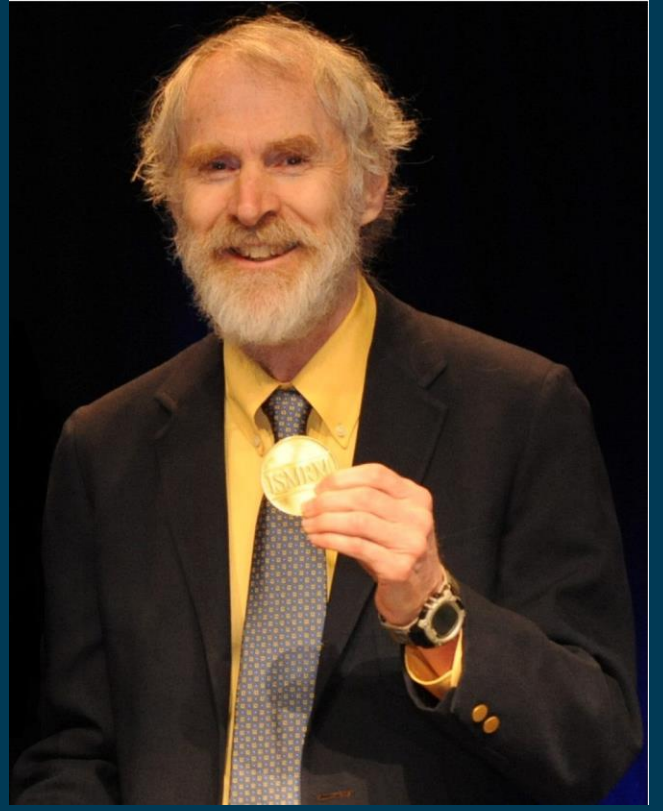

William Thomas Dixon (1945-2022)

Image caption: Tom Dixon receives the Gold Medal Award at the 2013 ISMRM Annual Meeting, Salt Lake City, Utah, USA.

Tom died on August 1, 2022, due to complications from Parkinson's disease.

The End